Thermal properties of thermoplastic starch/synthetic polymer blends with potential biomedical applicability

J. F. MANO[1,2], D. KONIAROVA[1,2], R. L. REIS[1,2]
[1]*Department of Polymer Engineering, University of Minho, Campus de Azurém, 4800-058 Guimarães, Portugal*
[2]*3B's Research Group, Biomaterials, Biodegradables and Biomimetics, University of Minho, Campus de Gualtar, 4710-057 Braga, Portugal*

Previous studies shown that thermoplastic blends of corn starch with some biodegradable synthetic polymers (poly(ε-caprolactone), cellulose acetate, poly(lactic acid) and ethylene-vinyl alcohol copolymer) have good potential to be used in a series of biomedical applications. In this work the thermal behavior of these structurally complex materials is investigated by differential scanning calorimetry (DSC) and by thermogravimetric analysis (TGA). In addition, Fourier-transform infrared (FTIR) spectroscopy was used to investigate the chemical interactions between the different components. The endothermic gelatinization process (or water evaporation) observed by DSC in starch is also observed in the blends. Special attention was paid to the structural relaxation that can occur in the blends with poly(lactic acid) at body temperature that may change the physical properties of the material during its application as a biomaterial. At least three degradation mechanisms were identified in the blends by means of using TGA, being assigned to the mass loss due to the plasticizer leaching, and to the degradation of the starch and the synthetic polymer fractions. The non-isothermal kinetics of the decomposition processes was analyzed using two different integral methods. The analysis included the calculation of the activation energy of the correspondent reactions.

1. Introduction

Starch is a biopolymer present, as minute granules, in the roots, seeds and stems of a variety of plants, including corn, wheat, rice, millet, barley and potatoes. Chemical and physical properties of starch have been widely investigated due to its suitability to be converted into a thermoplastic and then to be used in different applications as a result of its known biodegradability, availability and economical feasibility [1, 2].

Unfortunately, native starch has poor mechanical properties and is predominantly water-soluble and cannot be processed by melt-based routes without being degraded. In order to be able to compete with non-degradable plastics, blending or grafting starch with synthetic hydrophobic polymer has been suggested as a suitable route in improving properties [2–15]. Reactions with starch are facilitated by the presence of numerous hydroxyl groups. Further information on the structure of starch, its destructurization into a thermoplastic and its blending with synthetic polymers may be found in a review by Reis and Cunha [16]. Recently, different starch/synthetic polymer blends have been suggested to have potential for use in distinct biomedical applications. These include the use of starch-based biomaterials as scaffolds for the tissue engineering of bone and cartilage [17], materials for bone fixation and replacement as well as for filling bone defects [18, 19], carriers for the controlled release of drugs and other bioactive agents [20], and new hydrogels and partially degradable bone cements [21, 22]. Furthermore, it has been shown in several studies that these polymeric systems exhibit: interesting degradation kinetics [17, 23, 24]; an undoubtable biocompatible behavior [25, 26] that is not typical at all of biodegradable systems; and tailorable surface characteristics that can be adjusted to favor cell adhesion and proliferation [23, 26–28]. The structure at the molecular level of those blends is very complex, involving possibly interpenetrating networking or other chemical reaction during the blend of the components [16]. Therefore, an effort has been made in order to characterize the properties of such systems, which may be useful for the processing of the material and for the prediction of some features during their potential application as biomaterials.

In this work starch-based thermoplastic blends were studied. Different blends were selected being the synthetic polymer, the blend label (S is for starch) and respective amounts: (i) poly-(L-lactic acid), SPLA50 and

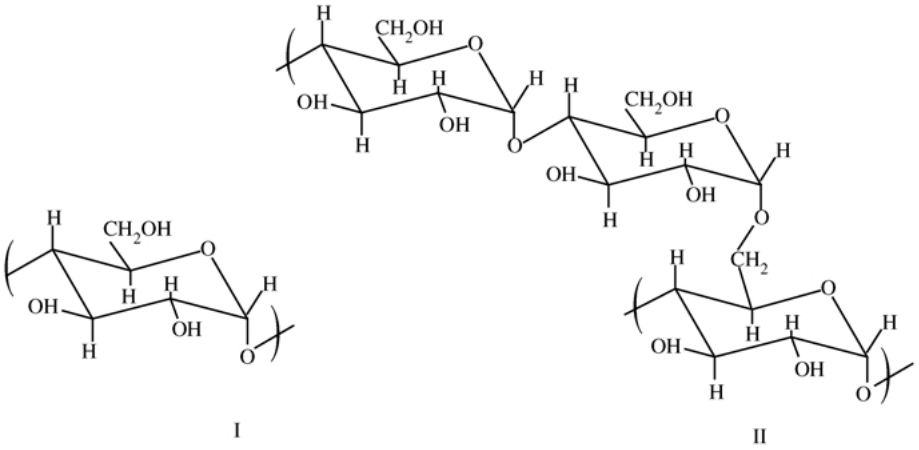

Figure 1 Structures of amylose (I) and amylopectin (II).

SPLA70, 50 and 70 wt %, (ii) poly(ε-caprolactone), SPCL, 70 wt %, (iii) cellulose acetate, SCA, 50 wt %, and an (iv) ethylene-vinyl alcohol copolymer, SEVA-C, 50 wt %. The blends were characterized by FTIR, differential scanning calorimetry (DSC) and thermogravimetry analysis (TGA). The two former techniques will provide informations about the possible chemical changes occurred in starch upon blending. DSC also provided information about the physical transitions that can take place in the materials. TGA is a suitable technique to study the thermal stability of polymer-based systems. For the particular systems analyzed in this work, the aim of the study was to obtain relevant information on the processability of the blends (in terms of their thermo-degradability) and to characterise their thermal degradation-kinetics.

2. Experimental

2.1. Materials

The starch-based thermoplastic blends studied in this work were supplied by Novamont, Novara, Italy. They included blends of (i) corn starch/ethylene-vinyl alcohol copolymer (SEVA-C, 50/50 wt %), (ii) corn starch/cellulose acetate (SCA, 50/50 wt %), (iii) corn starch/poly (ε-caprolactone) (SPCL, 30/70 wt %), (iii) corn starch/poly (L-lactic acid)-(50/50 wt %) (SPLA50) and (iv) corn starch/poly (L-lactic acid)-(30/70 wt %) (SPLA 70). The as-received materials appeared in a granular form. Prior to the experiments the blends were powdered in a high speed milling equipment.

In order to study the influence of blending, native Corn starch (from Cargill Bv, Holland) and poly(L-lactic acid) (Purasorb®PL, batch number BD742GL, from Purac, The Netherlands) were also analyzed.

2.2. Methods

The Fourier Transformed Infrared Spectroscopy (FTIR) spectra were recorded, at room temperature, in a Perkin Elmer System 1600 FTIR Spectrometer, with resolution of 2 cm^{-1} and averaged over 32 scans in the range 400–4000 cm^{-1}. Samples were thoroughly grounded with potassium bromide (KBr) and pellets were prepared by cold compression under vacuum.

DSC experiments were carried out in a Perkin Elmer DSC7 differential scanning calorimeter with controled cooling accessory. The temperature of the equipment was calibrated with indium and lead standards and for the heat flow calibration only indium was used, under the same conditions as for the samples. All materials were sealed in Aluminum pans and the DSC scans were performed in a temperature range of 25–220 °C at a heating rate of 10 °C min^{-1}. All scans were subtracted from a blank trace, obtained at the same conditions, with an empty pan.

Thermal degradation was measured using a Perkin Elmer TGA7 equipment under a nitrogen atmosphere. The experiments were performed at a 10 °C min^{-1} heating rate in the temperature range 25–550 °C. The initial weight of the samples were typically around 20 mg.

3. Results and Discussion

3.1. FTIR Spectroscopy

The chemical structure of starch consists of two polysaccharides: amylose (structure I in Fig. 1), mainly linear in structure, and a more branched structure, amylopectin (structure II in Fig. 1). Starch differs chemically from cellulose in two major ways: the glucose rings are linked by carbons 1 and 4 by α- rather β-linkages, and significant chain branching occurs through carbon 6. The more common molecular weight range for amylose is 200 000–300 000 and over 1 million for amylopectin.

The FTIR spectrum of pure starch is presented in Fig. 2, and the assignments of the main absorption bands of starch are indicated in Table I. The results are in accordance with the typical starch spectra obtained by other authors (e.g. Kweon *et al*. [29], Tikuisis *et al*. [30] and Park *et al*. [31]).

FTIR Spectroscopy was used to investigate possible differences between the spectra of starch and starch based blends, which could indicate changes in the chemical structure upon blending.

The spectra for the studied blends and for PLA are shown in Fig. 1. The presence of glycerol in the blends is smeared by the fact that its FTIR pattern is very similar to that of starch [31]. It is also possible to conclude that a low content of coordinated water molecules exists in the blends from the weak bands at 670 and 900 cm^{-1}, corresponding to the wagging (out-of-plane bending) and

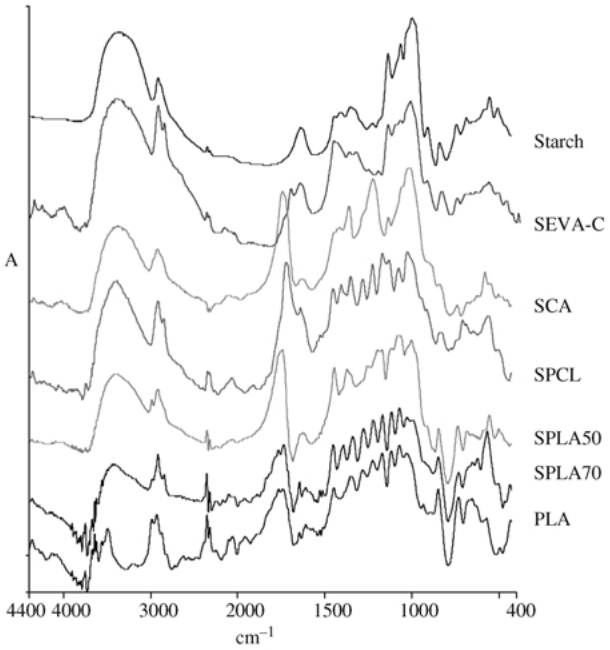

Figure 2 FTIR spectra of the studied blends, corn starch and PLA.

rocking vibrations of the –OH groups in water, respectively. Such conclusion is supported by the TGA results (see later in the text) where no evident decrease in the mass is observed just above 100 °C.

The sharp carbonyl absorption band specific to SCA, SPCL, PLA, SPLA 50, SPLA 70 is observed at 1730–1755 cm^{-1} [15, 29, 32]. The spectra of SPLA50 is more similar to the spectra of starch than SPLA70, which is closer to the PLA one, specially in the 100–1500 cm^{-1} region. This is simply a result of the different composition of starch and PLA in the blends.

The SCA spectra is consistent with what was observed by other authors [32] for cellulose triacetate where bands at 3683, 1755 and 1214 were detected, assigned to the hydroxy, ester carbonyl and ether carbon-oxygen groups, respectively.

3.2. Differential scanning calorimetry

The DSC traces of all the studied materials are shown in Fig. 3. The curves were separated in two sets, the upper ones being for the PLA-based materials.

The DSC trace of the native corn starch shows a broad endothermic peak from room temperature up to temperatures above 150 °C (onset temperature at 58.3 °C). The enthalpy of the process is 294.6 $J \cdot g^{-1}$. This peak was also observed by other authors [32], being assigned to the gelatinization of the material. In this

TABLE I Characteristic FTIR bands of native starch

Wavelength (cm^{-1})	Assignment	Ref.
3900–3300	O–H stretching	[29–31]
2920	C–H stretching	[31]
1640	δ(O–H) bend of water	[31]
1462	CH_2	[31]
1445–1325	C–H bending and wagging	[31]
1243	O–H bending	[31]
1250–900	C–O stretching	[15, 30, 31]

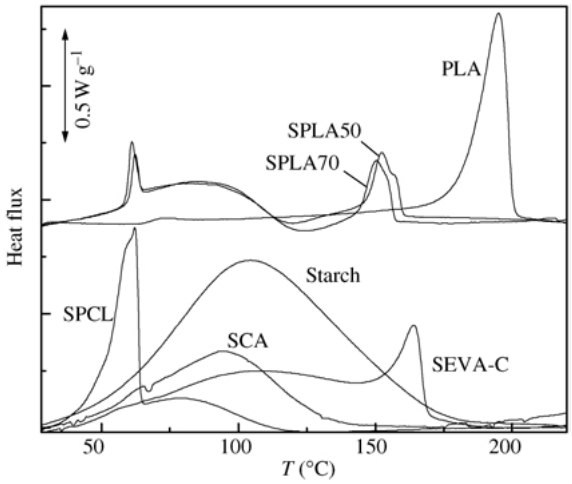

Figure 3 DSC thermograms obtained at 10 °C min^{-1} for the studied materials. Two groups of results are separated by vertical shifts for clarity.

process the typical granules observed in native starch (e.g. micrographs showing this morphology in Park *et al.* [31]) collapse while, at a molecular level, the hydrogen bonding are disrupted. It was found that the enthalpy of the transition strongly depend on the moisture content, and could vary from 119 Jg^{-1}, for 20 mass/v % of water content up to 395.8 $J \cdot g^{-1}$, for a water content of 50 mass/v % [33]. One could also attribute the observed endothermic peak to water adsorption that can occur above room temperature during heating. This assignment is consistent with the increase of the enthalpy with increasing water content [33]. This hypothesis is also in accordance with the TGA results (shown later in this text), which suggest the occurrence of water evaporation above room temperature. Other authors reported only a broad endothermic peak from 163 to 230 °C in dry powders of native starch (10% water content) [29]. In that case, the peak was attributed to both the melting of the starch crystals and to their thermal decomposition. This last hypothesis is inconsistent with the TGA results, which will be presented and discussed later, where the thermal degradation of starch is found at a higher temperature.

It must be noticed that the endothermic peak observed in the pure starch is always observed in the blends, but with a smaller area. For example, in the SCA blend, where no transitions are observed in the synthetic component, in the studied temperature range, the endothermic peak has an enthalpy of 104.3 $J \cdot g^{-1}$. This value is lower than the expected taking into account both the enthalpy found for the pure starch and the starch content in the blend, that is of ca. 50 wt %. However, it must be stated herein that the starch component in the blend and the pure starch are from different origins and that during the blend preparation there are obvious changes in the moisture content of the materials.

In the SEVA-C material one detects an endothermic peak that overlaps with the starch peak. This transition, with an onset at 153.9 °C and $\Delta H = 24.1\,Jg^{-1}$, is assigned to the melting of the ethylene-vinyl alcohol copolymer fraction.

The melting peak of the poly(ε-caprolactone) fraction in the SPCL blend is well visible in the DSC trace, with

an onset at 50.6 °C and an enthalpy of $49.7\,J \cdot g^{-1}$. Taking into account the melting enthalpy of $76.5\,J \cdot g^{-1}$ for 100% crystalline polycaprolactone, reported by Huang *et al*. [34], one can estimate the content of crystalline synthetic material in the blend as 65–70%. The glass transition of the poly(ε-caprolactone) in SPCL was not detected in the studied temperature window. Previous studies in a similar blend reported a T_g at − 66.4 °C and a melting temperature at 52.9 °C [35]. In this work the authors found a melting enthalpy of $27.7\,J \cdot g^{-1}$, a lower value than the one measured in this work.

The two blends with poly(L-lactic acid), SPLA50 and SPLA70, present two processes besides the peak assigned to the starch: a smaller peak at ∼ 60 °C and a more intense endothermic peak at 143.9 °C ($\Delta H = 12.4\,Jg^{-1}$) and 147.9 °C ($\Delta H = 14.3\,Jg^{-1}$) for SPLA50 and SPLA70, respectively. The DSC result for commercially available poly(L-lactic acid) may be helpful for further discussion. The obtained trace is also shown in Fig. 2 and clearly points out for a glass transition at 68.3 °C ($\Delta C_p = 0.20\,J \cdot K^{-1} \cdot g^{-1}$) and a melting peak at 182 °C ($\Delta H = 68.0\,Jg^{-1}$). Therefore the attribution of the high temperature peaks in the SPLA50 and SPLA70 blends to the melting of the crystalline fraction of the PLA is straightforward. As expected the melting heat for SPLA50 is lower than for the SPLA70 blend, due to the lower content of PLA. Moreover, one finds that the melting temperatures of the blends are much lower than for pure PLA. This may be a result of the constrains induced by the starch in the crystallization of PLA, leading to thinner lamellae than the ones produced in the pure PLA. The melting peak of the PLA fraction in SPLA50, which is the blend with higher starch content, shows a shoulder at higher temperatures, indicating a bimodal or broad lamellae thickness distribution. Moreover, the melting temperature of this blend is lower than for SPLA70. Again, this is a consequence of the influence of starch in the morphology development of PLA.

The transition appearing at ∼ 60 °C in SPLA50 and SPLA70 is assigned to the glass transition of the amorphous fraction of PLA. The endothermic peak is related with the structural relaxation of the polymer that occurred at room temperature during the storage time (between the processing and the experiments). In fact, the typical trace for the glass transition, without this endothermic peak, is obtained if the blends are previously heated at temperatures above 70 °C. This physical aging process is a general phenomena of glass forming materials [36] and is of particular relevance when PLA-based materials are used in biomedical applications. Due to the fact that the glass transition of this polymer is above but close to body temperature, a processed part (implant) cooled to body temperature undergoes a slow relaxation process where relevant physical properties, such as enthalpy, entropy or volume, tend towards their equilibrium values. An important consequence if a processed piece is implanted in the human body is that continuous physical changes occur in the material: for example, the volume tends to decrease, and, more important, the general mechanical properties may be deeply modified with time. To our knowledge extensive studies on the kinetics of structural relaxation in PLA are scarce but it was reported that this process may greatly effect the thermal properties of P(DLLA) [37].

The glass transition of the studied blends are 59.2 °C ($\Delta C_p = 0.37\,J \cdot K^{-1} \cdot g^{-1}$) and 59.6 °C ($\Delta C_p = 0.41\,J \cdot K^{-1} \cdot g^{-1}$) for SPLA50 and SPLA70, respectively. These values and the one found for the pure PLA are higher than the glass transition of amorphous P(DLLA) – composed by a copolymer of D- and L-lactic acid. For example, Jacobsen and Fritz [38] reported $T_g = 54$ °C for a pure amorphous PLA. This is consistent with the change of the molecular mobility when the amorphous fraction is located between crystalline lamellae, that is the case of a semicrystalline material, relatively to the amorphous situation. A similar discussion, for example, on DSC results with poly(ethylene terephthalate), which is also a polyester, with different crystallinity degrees may be found elsewhere [39].

3.3. Thermogravimetry

3.3.1. Results

TGA has proved to be a suitable method to investigate the thermal stability of polymeric systems [40]. The knowledge of degradation and mode of decomposition under the influence of heat is highly recommended in the processing optimisation. The threshold decomposition temperature gives an indication of the highest processing temperature that can be used, whereas the study of the kinetics of the different decomposition processes may help in the identification of the degradation mechanisms.

Usually, the analysis of TGA data is not straightforward. The rough results cannot be directly converted into absolute features of the studied material. In fact, they may depend of factors such as the sample geometry/mass, sample compactability, heating rate or gas environment. The results reported in this work are specific to the experimental conditions used. The comparison between the obtained results and data extracted from literature must be prudent. Precautions were taken to maintain the same geometry or mass of the different studied samples. Therefore, at least, a comparative analysis between the studied materials can be done.

The TGA results of the studied materials are shown in Fig. 4. As for the DSC data, the results are shown in two separated groups. In Fig. 4(a) the mass loss plots of starch, PLA and SPLA blends are shown and in Fig. 4(b), the corresponding derivative of the data (DTG) are shown. The same kind of plots are shown in Fig. 4(c) and (d) for the set of starch, SEVA-C, SCA and SPCL.

Fig. 4 suggests the occurrence of three weight loss processes: below 280 °C, between 280 and 350 °C and above 350 °C.

The initial weight loss process in the studied native starch, that starts just above room temperature, correspond to water desorption (DTG peak at ∼ 70 °C). This process was not observed in the blends, being an indication that a small quantity of water is adsorbed in their structures. In the SEVA-C, SCA and SPCL one detects a degradation process initiating at ca. 150 °C attributed, as other authors suggested [41], to the loss of

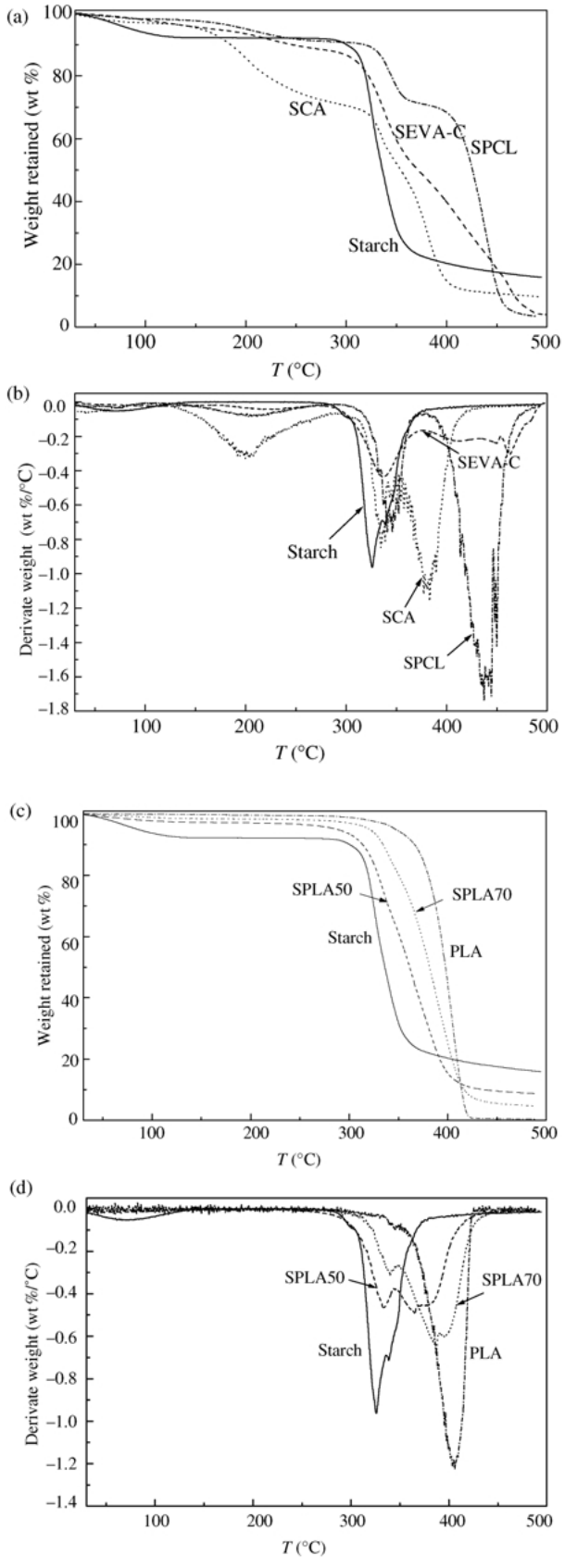

Figure 4 Thermogravimetry results on starch, SEVA-C, SCA and SPCL (a) TGA plots, (b) DTG plots, monitored at 10 °C min^{-1} under an atmosphere of flowing dry nitrogen. Thermogravimetry results on starch, SPLA50, SPLA70 and PLA (c) TGA plots, (d) DTG plots, monitored at 10 °C min^{-1} under an atmosphere of flowing dry nitrogen.

plasticizers (mostly glycerol). This weight loss is more visible in SCA and, surprisingly, is absent in SPLA50 and SPLA70.

The process at 280–350 °C is attributed to the degradation of the starch component. Native starch shows one, but complex, degradation step at 300–350 (peak in the derivative weight loss) and all the blends also present this process, at a slightly higher temperature. This shift in the temperature axis could be a result of the more complex nature of starch in the blends, probably forming interpenetrating networks structures with the synthetic polymer. The shoulder in the starch degradation peak was also observed by other authors [42] and may be due to the different degradation rate of amylose and amylopectin, the former being probably the first degraded due to its linear structure. A recent study also reported the starting of thermal reactions of starch around 300 °C [43]. NMR spectroscopy measurements allowed to detect both thermal condensation between hydroxyl groups, forming ether links, and de-hydration of neighboring hydroxyl groups in the glucose ring (causing ring scission or double-bond formation) [43]. At higher temperatures aromatic and even cross-linked structures are formed.

The processes observed in the blends above the degradation of starch are attributed to the pyrolysis of the synthetic component. This is well evident when this higher temperature process increases in magnitude and shifts to higher temperatures (tending to behave like for the pure PLA case) when one goes from SPLA50 to SPLA70. This third degradation process is less clearly seen in SEVA-C but it is documented in the literature [41].

The degradation extent and the peaks' positions of the derivative of the mass loss of all these three processes in all the studied materials are shown in Table II. Such kind of representation may be helpful in the quality control of the obtained products. For example, as PLA degrades almost completely, the mass loss during the higher degradation process of PLA50 and PLA70 gives a direct indication on the PLA content in the blends. In this work the degradation extent in PLA50 and PLA70 yield 57% and 75%, which is similar to the nominal PLA content in the blends (50 and 70 wt/wt %, respectively).

3.3.2. Kinetic analysis

The expression for the thermal decomposition of a homogeneous system has the following general form:

$$\frac{d\alpha(t)}{dt} = k(T)f[\alpha(t)] \qquad (1)$$

α represent the reaction extent of the component of the sample being degraded, defined by $\alpha(t) = (w_0 - w(t))/(w_0 - w_\infty)$, in which w_0, $w(t)$ and w_∞ are the weights of the sample before the degradation, at time t and after total conversion, respectively. $k(T)$ is the rate coefficient that usually follows the Arrhenius equation. The differential conversion function, $f(\alpha)$ may present various functional forms but its most commonly form for solid-state reactions is $f(\alpha) = (1-\alpha)^n$, where n is the reaction order, assumed to remain constant during the reaction [40].

At a certain heating rate $\beta = dT/dt$, we have

$$\frac{d\alpha}{(1-\alpha)^n} = \frac{A}{\beta}\exp\left(-\frac{E_a}{RT}\right)dT \qquad (2)$$

where E_a is the activation energy and A the Arrhenius pre-exponential factor. A large number of pyrolysis

TABLE II Temperature of maximum rate of mass loss (T_{max}) and degradation extent (DE) for the three degradation mechanisms observed in all studied materials

Temperature region	< 280 °C		280–350 °C		> 350 °C	
Sample	T_{max}/°C	DE%	T_{max}/°C	DE%	T_{max}/°C	DE%
STARCH	—	—	326	75	—	—
SEVA-C	220	7	338	40	412	44
SCA	203	25	335	20	380	42
SPLA 50	Not observed		332	30	364	57
SPLA 70	Not observed		340	17	388	75
PLA	—	—	—	—	404	99
SPCL	200	7	344	20	441	67

processes can be represented as first order reactions [44]. Particularly, the degradation of a series of unoxidised and oxidised starch was suggested to be first order in sample weight reaction [45]. Therefore we will assume $n = 1$ for the remainder of the present text. Under this assumption the integration of Equation 2 leads to:

$$\ln(1-\alpha) = -\frac{A}{\beta}\int_{T_0}^{T} \exp\left(-\frac{E_a}{RT'}\right) dT' \qquad (3)$$

The temperature integral does not have an exact form. Several approximations for the integrand function lead to several methods for evaluation of the thermokinetic parameters A and E_a from a single thermogravimetric experiment carried out at a given heating rate. Two methods that differ on the way of resolving Equation 3 are compared using the TGA data of the studied blends.

Horowitz and Metzger [46] suggested the use of an auxiliary temperature variable defined as $\theta = T - T_m$, where T_m is a temperature where $\alpha = (e-1)/e$, i.e. for a first order reaction T_m is the temperature of maximum degradation rate As $\theta/T_m < 1$ we may have:

$$\frac{1}{T} = \frac{1}{T_m(1+\theta/T_m)} \cong \frac{1-\theta/T_m}{T_m} \qquad (4)$$

This approximation allows to calculate the integral in Equation 3:

$$\ln(1-\alpha) = -\frac{A}{\beta}\frac{RT_m^2}{E_a}\exp\left[-\frac{E_a}{RT_m}(1-\theta/T_m)\right] \qquad (5)$$

When $T = T_m$ then $\theta = 0$ and $\ln(1-\alpha) = -1$. Under this condition Equation 5 turns to

$$-1 = -\frac{A}{\beta}\frac{RT_m^2}{E_a}\exp\left[-\frac{E_a}{RT_m}\right] \qquad (6)$$

The substitution of this equation in Equation 5 results in

$$\ln(1-\alpha) = -\exp\left(\frac{E_a\theta}{RT_m}\right)$$

or

$$\ln(-\ln(1-\alpha)) = \frac{E_a\theta}{RT_m} \qquad (7)$$

Thus, a plot of $\ln(-\ln(1-\alpha))$ against θ should give a straight line whose slope is E_a/RT_m [46]. This procedure for handle the experimental data is usually called the Horowitz-Metzger or HM method.

In the Broido method one assumes that $\exp(-E_a/RT) \cong (T_m/T)^2\exp(-E_a/RT)$ (i.e. the temperature range of analysis is close to T_m) [44]. Then the Equation 3 may be written as

$$\ln(1-\alpha) = -\frac{A}{\beta}\frac{RT_m^2}{E}\exp\left(-\frac{E_a}{RT}\right)$$

or

$$\ln(-\ln(1-\alpha)) = -\frac{E_a}{RT} + \text{const} \qquad (8)$$

In this method a straight line should be observed between $\ln(-\ln(1-\alpha))$ and $1/T$ with a slope of $-E_a/R$. The method described by Broido was successfully applied in polysaccharides-based materials. In this work all the blends will be analyzed under this method [47]. The HM method was also used in TGA studies on polysaccharides-based materials such as in a cellulose acetate hydrogen phthalate [48]. The weight loss processes will be also investigated with the HM method in order to verify if the simplification of the exponent in the integral of Equation 3 may effect the obtained activation energy.

The application of the Broido method for the starch, SEVA-C, SCA and SPCL series is shown in Fig. 5(a) and for the SPLA blends is shown in Fig. 5(b). The attempt was made to separate the three degradation processes in all formulations. For all the processes the $\ln(-\ln(1-\alpha))$ vs. $1/T$ plots in Fig. 5 are found reasonably linear.

The $\ln(-\ln(1-\alpha))$ vs. θ fits (Equation 7) were also carried out for all the three weight loss processes in all the materials. The application of this HM method in the description of the kinetics of the three loss mass processes in SPCL is exemplified in Fig. 6. It was also included in that Figure the degradation process of native starch. Also for this method good linear relationships were obtained.

The activation energies obtained by both the Broido and HM methods are presented in Table III. Considering the differences in the values of the activation energies when different processes or different materials are compared, it can be concluded that the differences observed due to the calculation method, for a particular process and material, are relatively small. Table III seems only to indicate a tendency for higher activation energies when calculated with the HM method. The same magnitude of differences was also observed when the activation energies of a series of materials obtained using the HM were compared with the ones obtained with another method (the Coats–Redfern method) [48].

As the region of the process occurs at higher temperature we observe that the corresponding activation energy also increases. This is an indication that as the energy barrier increases the weight loss process appears

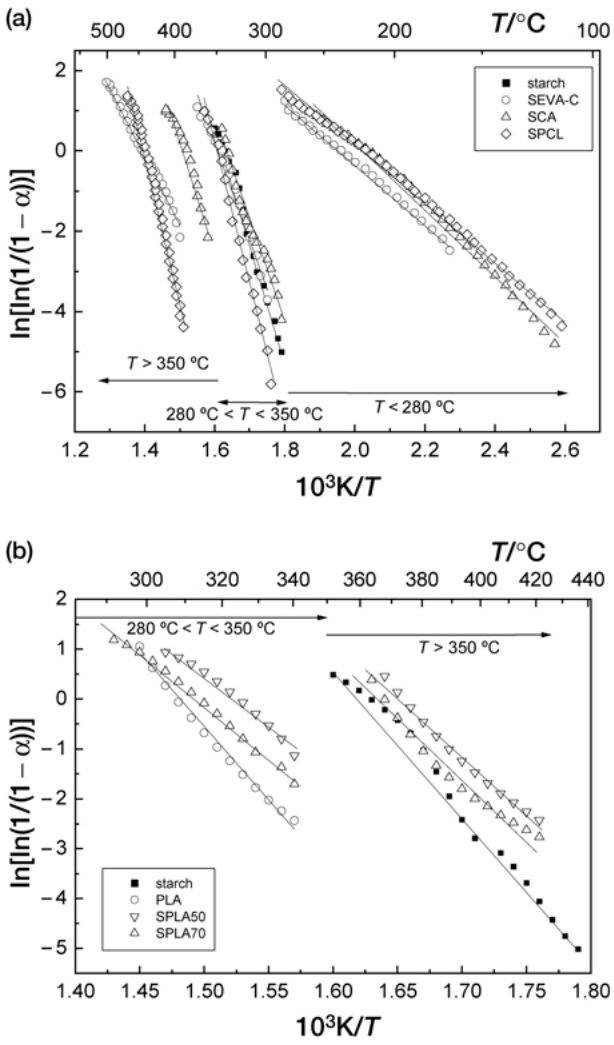

Figure 5 $\ln(-\ln(1-\alpha))$ vs. $1000/T$ plots using Broido method for (a) starch, SEVA-C, SCA and SPCL and (b) starch, SPLA50, SPLA70 and PLA.

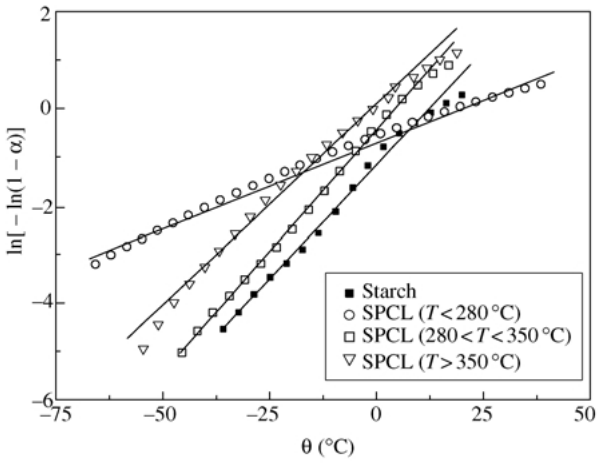

Figure 6 $\ln(-\ln(1-\alpha))$ vs. θ plots using the Horowitz-Metzger method for the degradation of starch (solid squares) and the three processes in SPCL (open symbols).

more stable, occurring at higher temperature. The exception is found for SEVA-C, where entropic reasons may be associated.

The activation energy of the low degradation process does not depend on the material, giving values around 62–67 kJ mol^{-1}. This is due to the fact that the loss of plasticizer is a process that depends weakly on the matrix, at least for the series of synthetic polymers incorporated in the blends that were analyzed. The degradation of starch occurs with very distinct activation energies, depending on the blend, ranging from ∼150 kJ mol^{-1} for SPLA70 to more than ∼300 kJ mol^{-1} for SPCL. This may be an indication of different chemical affinities between starch and the synthetic polymer that may influence the pyrolysis process of starch. The degradation of the synthetic polymers (above 350 °C) also occurs with distinct activation energies, which will depend on their chemical structure. The composition may also have an influence on such values. For example the activation energy of PLA is ∼330 kJ · mol^{-1}. A decrease to ∼190 kJ mol^{-1} is observed for SPLA70 followed by a further decrease to ∼170 kJ · mol^{-1} for SPLA50, that has more starch. This suggests that the residues of the degradation of starch tend to stabilize the degradation of PLA, or that the crystallinity of the PLA fraction are different in the various materials, influencing the degradation mechanism. More complementary studies should be performed in order to clearly understand such differences.

4. Conclusions

Several starch-based blends aimed at different biomedical applications were investigated by means of using

TABLE III Activation energies calculated by Broido and HM for native corn starch, PLA and the studied starch blends

Sample	Method	Activation energy (kJ/mol), temperature region/°C		
		< 280	280–350	> 350
STARCH	Broido	—	270	—
	HM	—	280	—
SEVA-C	Broido	62	203	147
	HM	63	223	125
SCA	Broido	70	225	240
	HM	78	224	244
SPCL	Broido	61	300	330
	HM	68	320	346
SPLA 50	Broido		159	171
	HM		159	172
SPLA 70	Broido		137	190
	HM		151	189
PLA	Broido	—	—	243
	HM	—	—	253

different characterization techniques such as DSC and TGA. The thermal analysis characterization DSC and TGA) was complemented with FTIR. The results allow to draw the following conclusions:

1. The position of the FTIR bands of the different vibrational modes in the blends and in the pure components are similar, indicating small chemical changes induced upon blending of corn starch with the distinct synthetic polymers.

2. The endothermic first-order-like process occurring in starch on heating, starting at room temperature, also takes place in the blends during heating, although with less intensity, probably due to the less water content in the blends.

3. The melting behavior of PLA is clearly altered when blended with starch. The glass transition of PLA is above but close to body temperature, also when blended with starch. Therefore PLA-based biomaterials may undergo slow but important physical changes with time when implanted into the body. This issue has not been properly addressed in the literature, and has not been identified as a reason for some concern when using PLA based biomaterials.

4. Three main thermo-degradation processes are found in the studied materials being assigned, with increasing temperature, to the volatilization of the plasticizer, to the pyrolysis of starch and to the pyrolysis of the synthetic polymer. During processing by extrusion or injection molding such materials are subjected to high temperatures (above 160 °C), pressure and shear stresses. Therefore the lower temperature process surely occurs and possibly the degradation of starch may emerge to some extent for more extreme processing conditions. This will have consequences on the physical properties and on the biological response when this material is implanted.

5. Both Broido and Horowitz-Metzger approaches permitted to study the kinetics of the weight-loss processes of the materials, giving consistent activation energy values.

As a general conclusion it might be said that the thermal properties of the starch based biomaterials, together with their damping properties [49], might allow for their use on several of the proposed biomedical applications thus avoiding the referred to problem of unexpected and unpredictable physical changes that can happen to PLA based biomaterials when implanted in the human body. Starch based polymers also combine a much cheaper price with a clearly better biocompatible behavior as shown in previous works.

References

1. ''Starch Chemistry and Technology,'' 2nd edn, edited by R. L. Whistler, J. N. Bemiller, E. F. Paschall (Academic Press, New York, 1984).
2. A. H. KHALIL, *Food Chem.* **68** (2000) **61**; J. S. PEANASKY, J. M. LONG and R. P. WOOL, *J. Polym. Sci.: Polym. Phys.* **29** (1991) 565.
3. F. H. OTEY, A. M. MARK, C. L. MEHLTRETTER and C. R. RUSSEL, *Ind. Eng. Chem. Prod. Res. Des.* **13** (1974) 90.
4. G. F. FANTA, R. C. BURR, W. C. DOANE and C. R. RUSSEL, *Starch/Starke* **30** (1978) 237.
5. E. B. BAGFEY, G. R. FANTA, R. C. BURR, W. C. DOANE and C. R. RUSSEL, *Polym. Eng. Sci.* **17** (1977) 311.
6. R. G. PATIL and G. R. FANTA, *Starch/Starke* **46** (1994) 142.
7. G. J. L. GRIFFIN, *Adv. Chem. Ser.* **134** (1974) 159.
8. E. R. GEORGE, T. M. SULLIVAN and E. H. PARK, *Polym. Eng. Sci.* **34** (1994) 17.
9. G. F. FANTA, C. L. SWANSON and R. L. SHOGREN, *J. Appl. Polym. Sci.* **44** (1992) 2037.
10. C. L. SWANSON, R. L. SHOGREN, G. F. FANTA and S. H. IMAM, *J. Environ. Polym. Degrad.* **1** (1993) 155.
11. M. F. KOENIG and S. J. HUANG, *Polymer* **36** (1995) 1877.
12. R. S. LENK, *ibid.* **21** (1981) 371.
13. Z. YANG, M. BHATTACHARYA and U. R. VAIDYA, *ibid.* **37** (1996) 2137.
14. Y. TOKIWA, A. IWAMOTO and M. KOYAMA, *Polym. Mat. Sci. Eng* **63** (1990) 742.
15. D. RAGHAVAN and A. EMEKALAM, *Polym. Degr. Stab.* **72** (2001) 509.
16. R. L. REIS and A. M. CUNHA, in ''Encyclopedia of Materials: Science and Technology'' (Elsevier Science Ltd, 2001) p. 8810.
17. M. E. GOMES, A. S. RIBEIRO, P. B. MALAFAYA, R. L. REIS and A. M. CUNHA, *Biomaterials* **22** (2001) 883.
18. R. L. REIS and A. M. CUNHA, *Journal of Applied Medical Polymers* **4** (2000) 1.
19. R. A. SOUSA, J. F. MANO, R. L. REIS, A. M. CUNHA and M. J. BEVIS, *Polym. Eng. Sci.* **42** (2002) 1032.
20. P. B. MALAFAYA, C. ELVIRA, A. GALLARDO, J. SAN ROMÁN and R. L. REIS, *J. Biomater. Sci.: Polym. Ed.* **12** (2001) 1227.
21. C. ELVIRA, J. F. MANO, J. SAN ROMÁN and R. L. REIS, *Biomaterials* **23** (2002) 1955.
22. I. ESPIGARES, C. ELVIRA, J. F. MANO, B. VASQUEZ, J. SAN ROMAN and R. L. REIS, *ibid.* **23** (2002) 1883.
23. D. DEMIRGÖZ, C. ELVIRA, J. F. MANO, A. M. CUNHA, E. PISKIN and R. L. REIS, *Polym. Degrad. Stability* **70** (2000) 161.
24. C. M. VAZ, A. M. CUNHA and R. L. REIS, *Materials Research Innovations* **4** (2001) 375.
25. S. C. MENDES, Y. P. BOVELL, R. L. REIS, A. M. CUNHA, J. D. DE BRUIJN and C. A. VAN BLITTERSWIJK, *Biomaterials* **22** (2001) 2057.
26. M. E. GOMES, R. L. REIS, A. M. CUNHA, C. A. BLITTERSWIJK and J. D. DE BRUIJN, *ibid.* **22** (2001) 1911.
27. I. B. LEONOR, A. ITO, K. ONUMA, N. KANZAKI and R. L. REIS, *ibid.* (2002), in press.
28. I. B. LEONOR, R. A. SOUSA, A. M. CUNHA, Z. ZHONG, D. GREENSPAN and R. L. REIS, *J. Mater. Sci.: Mater. Medicine* **13** (2002) 1.
29. D. K. KWEON, D. S. CHA, H. J. PARK, S. T. LIM, *J. Appl. Polym. Sci.* **78** (2000) 986.
30. T. TIKUISIS, D.E. AXELSON and A. SHARMA, *Polym. Eng. Sci.* **33** (1993) 26.
31. J. W. PARK, S. S. IM, S. H. KIM and Y. H. KIM, *Polym. Eng. Sci.* **40** (2000) 2539.
32. A. A. HANNA, A. H. BASTA, H. EL-SAIED and I. F. ABADIR, *Die Angewandte Makromolekulare Chemie* **260** (1998) 1.
33. F. S. SOUSA, A. P. G. BARRETO and R. O. MACÊDO, *J. Therm. Anal. Cal.* **64** (2001) 739.
34. S. J. HUANG, M. F. KOENIG and M. HUANG, in ''Biodegradable Polymers and Packaging,'' edited by C. Ching, D. L. Kglum and E. L. Thomas (Technomic Lancaster, PA, 1993), pp. 97–110.
35. M. DAY, J. D. COONEY, K. SHAW, J. WATTS, *J. Therm. Anal.* **52** (1998) 261.
36. See, for example, U. W. Gedde, ''Polymer Physics'' (Chapman & Hall, London, 1995), Ch. 5.
37. K. LIAO, D. QUAN and Z. LU, *Eur. Polym. J.* **38** (2002) 157.
38. S. JACOBSEN and H. G. FRITZ, *Polym. Eng. Sci.* **36** (1996) 2799.
39. N. M. ALVES, J. F. MANO, E. BALAGUER, J. M. MESEGUER DUEÑAS and J. L. GÓMEZ RIBELLES, *Polymer* **43** (2002) 4111.
40. T. HATAKEYAMA and F. X. QUINN, ''Thermal analysis,

Fundamentals and Applications to Polymer Science'' (John Wiley & Sons, Chichester, 1994).
41. D. VEGA, M. A. VILLAR, M. D. FAILLA, E. M. VALLÉS, *Polym. Bull.* **37** (1996) 229.
42. P. AGGARWAL and D. DOLLIMORE, *Thermoch. Acta.* **291** (1997) 65.
43. X. ZHANG, J. GOLDING and I. BURGAR, *Proceedings of the 7th World Conference on Biodegradable Polymers & Plastics, Pisa, Italy, June 4–8*, (2002) p. 131.
44. A. BROIDO, *J. Polym. Sci.*: A-2, **7** (1969) 1761.
45. A. A. SOLIMAN, N. A. EL-SHINNAWY and F. MOBARAK, *Thermoch. Acta* **296** (1997) 149.
46. H. H. HOROWITZ and G. METZGER, *Anal. Chem.* **35** (1963) 1465.
47. X. QU, A. WIRSÉN, A.-C. ALBERTSSON, *Polymer* **41** (2000) 4841.
48. R. V. RAO, P. V. ASHOKAN and M. H. SHRIDHAR, *Polym. Degrad. Stabil.* **70** (2000) 11.
49. J. F. MANO, R. L. REIS and A. M. CUNHA, ''Dynamic Mechanical Analysis in Polymers for Medical Applications,'' to appear in the Nato Science Series, Polymer Based Systems on Tissue Engineering, Replacement and Regeneration (Kluwer Academic Publishers, 2002).

Received 1 February
and accepted 25 July 2002